CHAPTER II

A NEW METHOD FOR DETERMINING THE TWIST ELASTIC CONSTANT OF NEMATIC LIQUID CRYSTALS

As discussed in the previous Chapter a twist deformation in a homogeneously aligned nematic liquid crystal taken between two plane glass plates does not reveal itself optically when observations are made in a direction normal to the sample film (fig. 2.1) For this reason, only a few attempts have been made in the past, *to* determine k_{22}. We shall summarise these in the following section.

Earlier methods used for measuring k_{22}

Of the different methods used so far only the first three listed below are capable of yielding accurate results. For the sake of completeness we have briefly mentioned the, other methods also.

1) Freedericksz and Zwetkoff (1934) allowed the light to fall at a Large angle on a homogeneously aligned sample between a convex lens and a prism. When a sufficiently strong magnetic field is applied

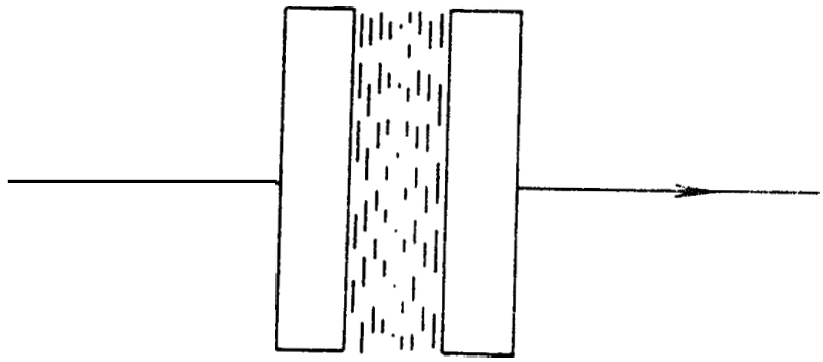

(a)

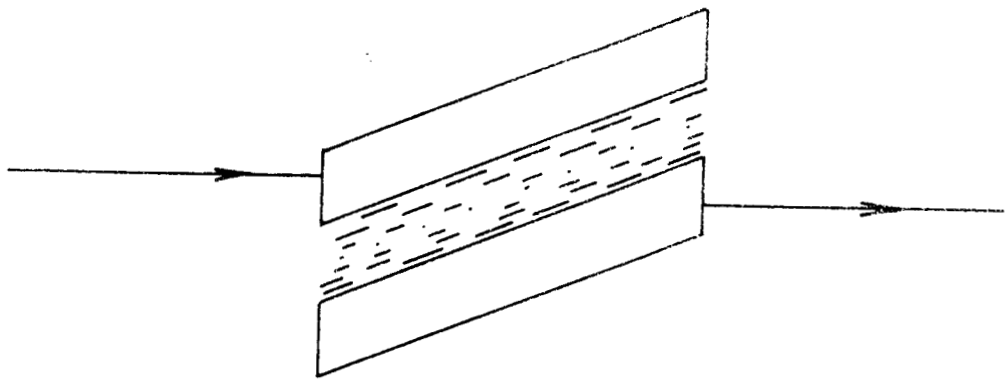

(b)

Figure 2*1

(a) Sample with twist deformation in the conventional geometry. The arrow shows the direction of light propagation.
(b) The new geometry: light falls on the sample film at an oblique angle.

normal to the director, the twist deformation occurs for a thickness greater than a critical value, $x_0(H)$ given by the equation (1.12), i.e., $H_c = \frac{\pi}{x_0}\left(\frac{k_{22}}{\Delta\chi}\right)^{\frac{1}{2}}$. The deformation increases as one moves away from the centre this being due to the increasing sample thickness. The central circular ares (with a thickness $< x_0(H)$ is undeformed. As we move away from the border between distorted and undistorted regions of the sample, the effective extraordinary refractive index decreases due to the increasing deformation. As a result total internal reflection takes place for a light beam (with proper polarization) incident obliquely on the border. By observing the totally reflected beam they could study the deformation in the sample and hence could determine $x_0(H)$ for an applied magnetic field. Using equation (1.12) k_{22} could then be calculated.

The method is quite good. But it requires the sample of varying thickness to be aligned and involves the measurement of angles and refractive indices. The method has not been used by later workers.

2) Cladis (1972) used a conoscopic figure method to determine H_c of a homogeneously aligned sample. A convergent beam of light is allowed to

fall on the sample to get a conoscopic figure (a pair of rectangular hyperbolae with one asymptote parallel 30 the undistorted director). When a magnetic field $H > H_c$ is applied in the plane of the plates and normal to the undistorted $\vec{n}$, the interference figure rotates by an mount δ given by (de Gennes 1974)

$$\tan 2\delta = \frac{\overline{\sin 2\theta}}{\overline{\cos 2\theta}} \qquad (2.1)$$

where θ is the local tilt of the optic axis induced by H. The averaging is done aver the thickness of the sample. H_c is obtained by extrapolating for zero δ.

This method is claimed to be quite accurate and has been wed now to get k_{22} over a range of temperatures (Leenhouts et al.).

3) Delaye et al.(1973) used the light scattering technique to determine the twist constant. Nematic liquid crystals are turbid and strongly scatter light. de Gennes (1968a) hau interpreted this strong scattering in terms of small amplitude orientational fluctuations of the director. By measuring the scattered intensity elastic constants can be determined (Orsay Liquid Crystal Croup 1969). Light is incident on a homeotropically aligned sample. $\vec{k}_e$ is the incident wave vector. (The

subscript e indicates the polarization setting corresponding to the extraordinary index.) Let $\vec{k}_o^s$ be the scattered wave vector. $\vec{k}_o^s$ is so chosen that the momentum transfer $\vec{q} = \vec{k}_e - \vec{k}_o^s$ is normal to the director. Then the intensity of scattering is due to twist fluctuations:

$$I \propto \frac{\varepsilon_a^2 T}{k_{22} q^2} \qquad (2.2)$$

where T is tho absolute temperature $\varepsilon_a = n_e^2 - n_o^2$ (n_e and n_o are the extraordinary and ordinary refractive indices).

This method can give accurate relative values and has been used in a few *recent* experiments (Chu and McMillan 1975, Delaye 1976).

4) Durand *et al.* (1969) applied a magnetic field normal to the twist &%xdf)~a nematic liquid crystal doped with a chiralic impurity so that a transition from cholesteric to nematic takes place at a certain critical field H_u. An equation relating to H_u and k_{22} has been given by de Gennes (1968b) and by Meyer (1968).

Some measurements have been carried out using this technique (PAA & PAP, Durand et al. 1969; MBBA,

Williams and Cladis 1972). However the error is quite large ($\sim \pm 15\%$).

5) Leslie (1970) derived a formula for the critical field required to distort a twisted nematic when the field is applied along the twist axis. The formula contains all the three elastic constants. Gerritsma *et al.*(1971) used the capacitance measurement to detect the critical field.

The method needs the values of other elastic constants and hence the error in k_{22} includes the errors in the measurements of k_{11} and k_{33}.

6) Leger (1972) measured the migration time τ of twist walls formed in a nematic drop placed in a rotating magnetic field. de Gennes (1971) has given a relation between τ and k_{22}. Experiments have been made on MBBA and PAA and the error involved in the method is quite large ($\sim \pm 15\%$) (Leger 1972).

7) Rondelez and Hulin (1972) applied a magnetic field along the twist axis of a nematic liquid crystal doped with a cholesteric compound and observed the Helfrich deformation (Helfrich 1970) which occurs beyond a certain critical field H_H. k_{22} can be obtained from this (Hurault 1973).

The method gives very low values of k_{22} ($\sim$ 50% lower than that obtained from other methods).

8) Haller (1972), following a suggestion by Meyer (1971) applied a magnetic field normal to the undistorted $\vec{a}$ and observed that beyond a critical field the electrohydrodynamic flow pattern rotates. However the method gives only an upper limit to k_{22} and not its actual value.

Recently Dreher (1974) suggested an oblique incidence method for the measurement of k_{22}. H_c is calculated by analysing the transmitted and reflected light. However no experiments appear to have been done using this method.

We have developed (1973) a simple technique of detecting the critical field in the case of twist deformation. We shall describe this method below.

The method

Consider a homogeneously aligned nematic liquid crystal between two plane glass plates. We can think of the sample *to* be divided into a number of thin sections parallel to the glass plates. If the deformation in the sample is weak, the twist per layer, β is very small compared to the phase retardation per layer

between the extraordinary and the ordinary rays. In such cases it is difficult to optically detect the twist for light propagating along the twist axis for reasons discussed in the previous chapter. However, by sending light at a suitable angle to the twist axis a and β can be made comparable in their magnitudes. Under euch circumstances it is possible to detect H_c by an optical method.

Near H_c the deformation and hence β is small. We can effectively reduce α by viewing the index ellipsoid at an oblique angle, say at $\approx 5°$ La the director. In such a case the effective extraordinary refractive *index* is given by the equation (fig.2.1b)

$$\frac{1}{n_{eff}^2} = \frac{\sin^2 \theta}{n_e^2} + \frac{\cos^2 \theta}{n_o^2} \qquad (2.3)$$

where θ is the angle between the director and the direction of observation. Under these conditions $\frac{\alpha}{=} \sim 4$ *or* 3 and *the* effective sample thickness also increases because of obliquity. The state of polarization of the light beam as it traverses the sample at this angle can again be understood from the Poincare sphere (fig. 2.2).

Let P represent the incident polarization as

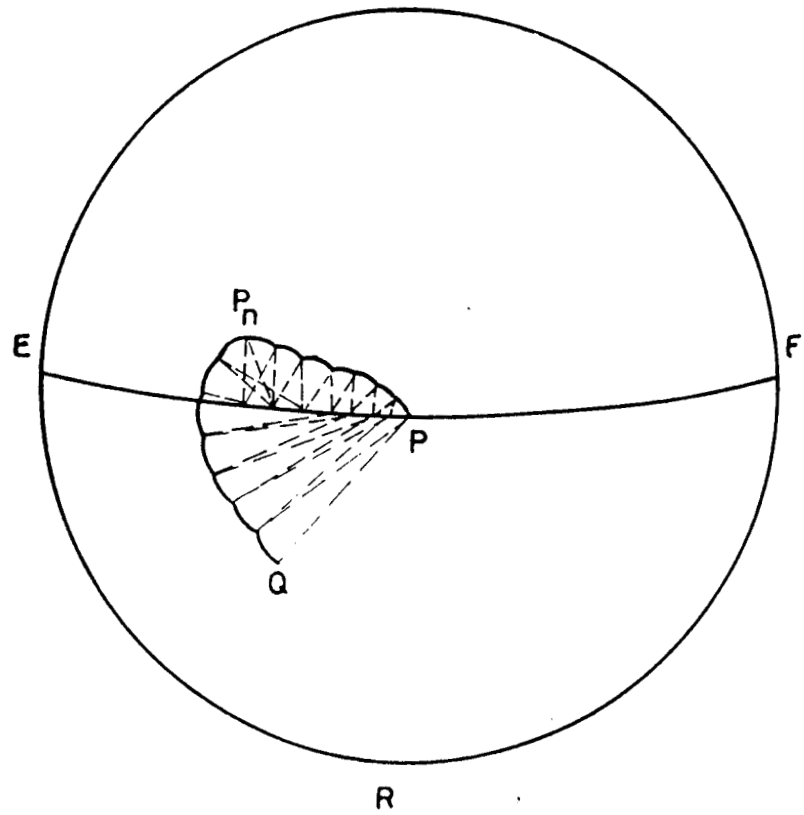

(a)

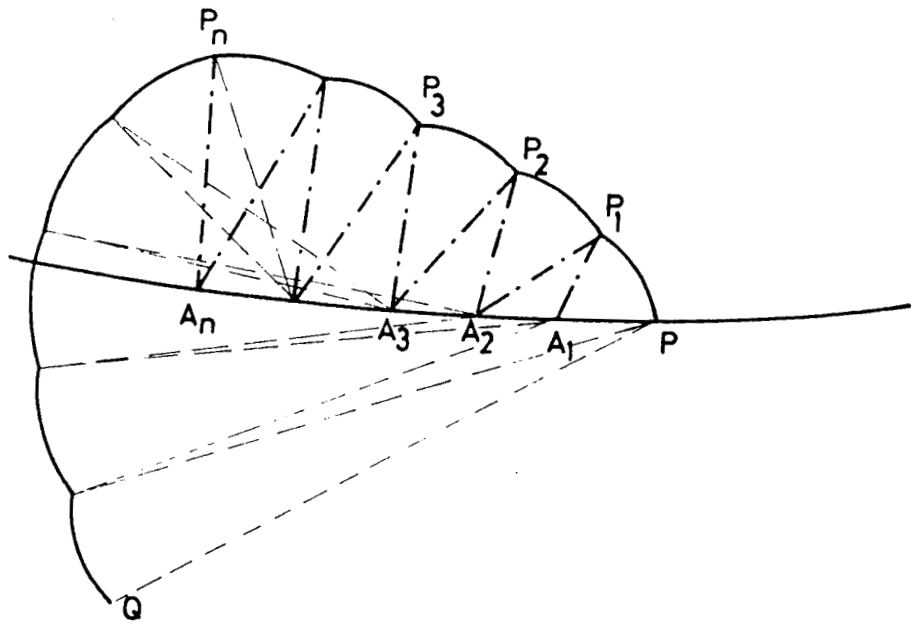

(b)

Figure 2.2: (a) Poincare sphere construction showing the state of polarization as light traverses the sample in the new geometry of figure 2.1b. The construction is shown in greater detail in (b). PA_1, A_1A_2 etc. represent the twist per layer. $\angle PA_1P_1$, $\angle P_1A_2P_2$, etc. represent the retardation per layer.

well as the director $\vec{n}$, as the light enters the sample. Consider the case where a small distortion has already taken plaoe. The operation on the Poincare sphere is described in detail in Chapter I. Now each section produces a phase retardation of comparable magnitude with the twist per layer. Q represents the polarization as the light emerges out of the sample. In the undistorted sample, the state of polarization of the emergent beam continues to be represented by P. Hence it is clear that tho stats of polarization is different from that in the undistorted sample. Such a change can easily be detected optically.

The experimental set up used to determine k_{22} using this method is given below.

Experimental arrangement

(a) Oven: A sketch of the oven is shown in figure 2.3a. A nichrome tape is wound uniformly round a long hollow copper cylinder (with a layer of mica for insulation). This is enclosed in another hollow cylinder of copper. The space between the two is filled by asbestos powder to reduce the radiation loss. The oven is heated by lead accumulators, the current being controlled by means of rheostats. Tho use of accumulators eliminated the problem of any fluctuations

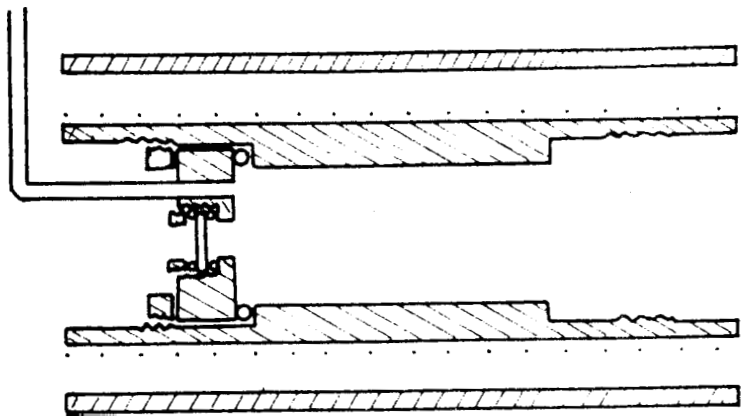

(a)

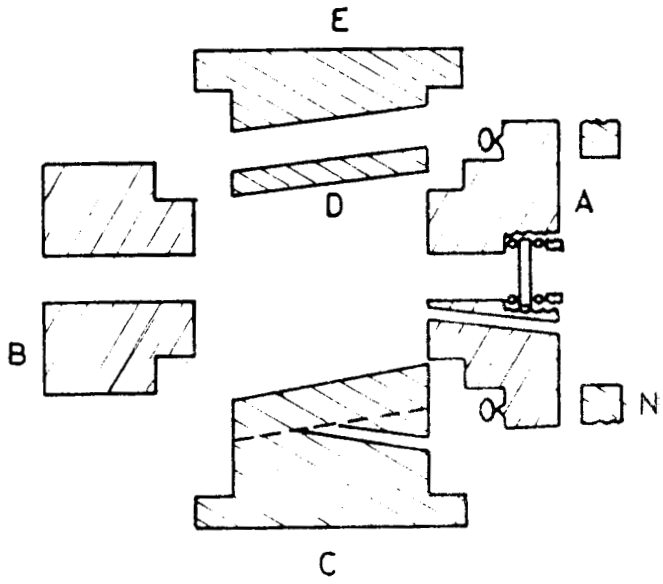

(b)

Figure 2.3

(a) Cross-sectionel diagram of the heater used. Striped areas represent copper.

(b) Different parts of the sample holder shown separately. (For explanation see text.)

in the mains. Moreover, since the oven is to be placed in a magnetic field, a direct current is preferable to A C. which sets up vibrations of the current carrying wire when the magnetic field is switched on.

The length of the oven is about 14 cms, whereas the glass plates holding the sample are only 2.5 cm long. These plates are mounted in a massive copper block, the length of which is 8.5 cm. The length of the oven is deliberately made much longer so that the temperature gradient along the length of the sample is minimised.

One end of the oven is closed by a one centimetre thick copper block with a central hole containing a glass window for observations. An inlet/outlet tube enables the chamber to be evacuated and filled with nitrogen (figure 2.3a).

(b) Sample holder: The sample holder consists of 5 parts (figure 2.3b). The part A contains a glass window and a hole to insert the hot junction of a thermocouple. This hole is continued in part C. In this block (C), a rectangular groove (indicated by dotted line) is out at an angle of $\approx 5°$ to the axis of the cylinder. The sample is contained between two

optically flat glass plates. The shorter edges of the glass plates are out and polished at 5° to the normal to the plates (*figure* 2.1b) such that the cross section parallel to the length and normal to the breadth is a parallelogram. The glass plater, placed in the groove can be held tightly by screwing on a rectangular copper plate D to C. This has a rectangular hole out in It to enable an optical measurement of the thickness of the sample. Part E joined with part C forms a cylinder. All the parts of the sample holder are held together by means of brase screws. The whole assembly (B, E + C and A) can be introduced into the oven and the space inside the oven made air tight using teflon washers and a nut N which locks into the right hand end of the oven shown in figure 2.3a.

(c) Sample preparation; Chatelain's rubbing technique was used for aligning the sample homogeneously (Chatelain 1943). For a good alignment, the glass surfaces should be absolutely clean (even a slight amount of grease favours homeotropic alignment). The glass plates were first washed in distilled trichloro-ethylene to remove any traces of grease. They were then kept in strong chromic acid for about 15 minutes. The oleaning process could be hastened by using warm

chromic acid. Finally they were rimed thoroughly in distilled water. The surface quality was tested by ensuring that a film of water sticks to the glass surface uniformly.

A clean filter paper (Whatman No.1) was uesd to rub the optically flat surfaces of the dried glass plats in a direction parallel to the length of the plates. While assembling the glass plates, care was taken to ensure that there was no relative tilt between the directions of rubbing of the two plates.

The glass plates were placed one over the other with two strips of spacer (mylar or mica) in between them. They were held tightly by part D of the sample holder. To ensure uniformity in the thickness of the air film between the glass plates interference fringes were formed in a light beam reflected from the two glass surfaces. The screws were tightened until straight fringes as few in number as possible are seen.

(d) <u>Thickness measurement</u>: Since the equation for the calculation of k_{22} involves the square of the sample thickness, it is necessary to measure it precisely. It is always found that the actual thickness of the sample is slightly larger than the nominal thickness of the spacer used.

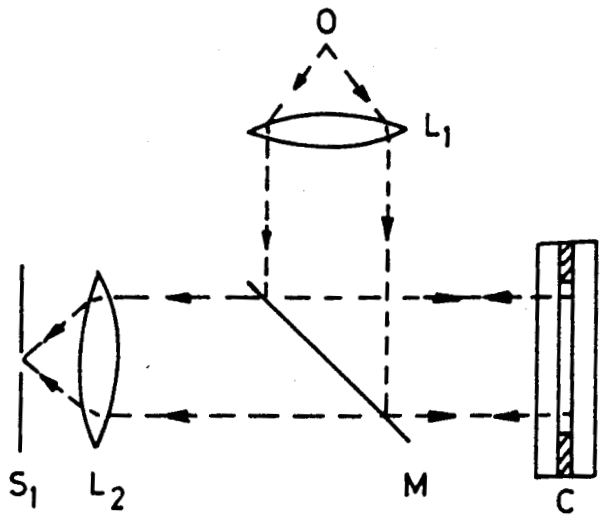

Figure 2.4

Arrangement to measure the thickness of the sample by forming the channelled spectrum.

The thickness of the sample was measured by using the channelled spectrum technique (see e.g., Ditchburn 1952) (figure 2.4). Light from a white light source O is rendered parallel by lens L_1 and is allowed *to* fall normally on tho air film between the glass plates. The light reflected from the air film is allowed to converge on the slit S_1 of a constant deviation spectroscope (Adam and Hilger Ltd.). In the field of view of the telescope, bright and dark bands are seen due to the interference of the light reflected from the two surfaces forming the air film. The thickness of the air film is given by

$$x_o = \frac{m \lambda_m \lambda_o}{2(\lambda_o - \lambda_m)} \qquad (2.4)$$

where λ_o is the wavelength corresponding to any dark fringe (say zeroth fringe) and λ_m that for m^{th} dark fringe.

(e) <u>Alignment of the director with respect to the magnetic field</u>: From equations (1.5) and (1.6) it is clear that the magnetic torque $\vec{\tau}_m = 0$ when n is parallel or perpendicular to $\vec{H}$ and the magnetic energy density is least when $\vec{n}$ is parallel to $\vec{H}$. A critical field exists only if the undistorted

director is exactly normal to . If $\vec{n}$ is slightly off-normal, distortion exists even for very small values of H so that a tail is formed near the critical field as shown from the calculations *of* Rapini and Papoular (1969).

To adjust $\vec{n}$ to be exactly normal to $\vec{H}$, the oven is mounted on a base provided with levelling screws L_1, L_2 and L_3 (figure 2.5a). It la also provided with side screws S_1 and S_2 having graduated heads. By using L_2 and L_3, the magnetic field was made to act In the plane of the nematic film. This adjustment ensures that *the* deformation is a pure twist. By using screws S_1 and S_2, $\vec{d}$ could be made exactly normal *to* $\vec{H}$. When $\vec{n}$ is exactly perpendicular to $\vec{H}$ there is no particular preference for the director *to* tilt in either direction from its undistorted orientation. As a result, regions *of* opposite twist separated by inversion walls are formed. Hence the screws S_1 and S_2 could be adjusted until the maximum number of such walls are observed.

(f) Temperature measurement and control: The temperature was measured using a copper-constantan thermocouple calibrated against a standard thermometer provided with the microheating table 'BOETIUS' (Franz

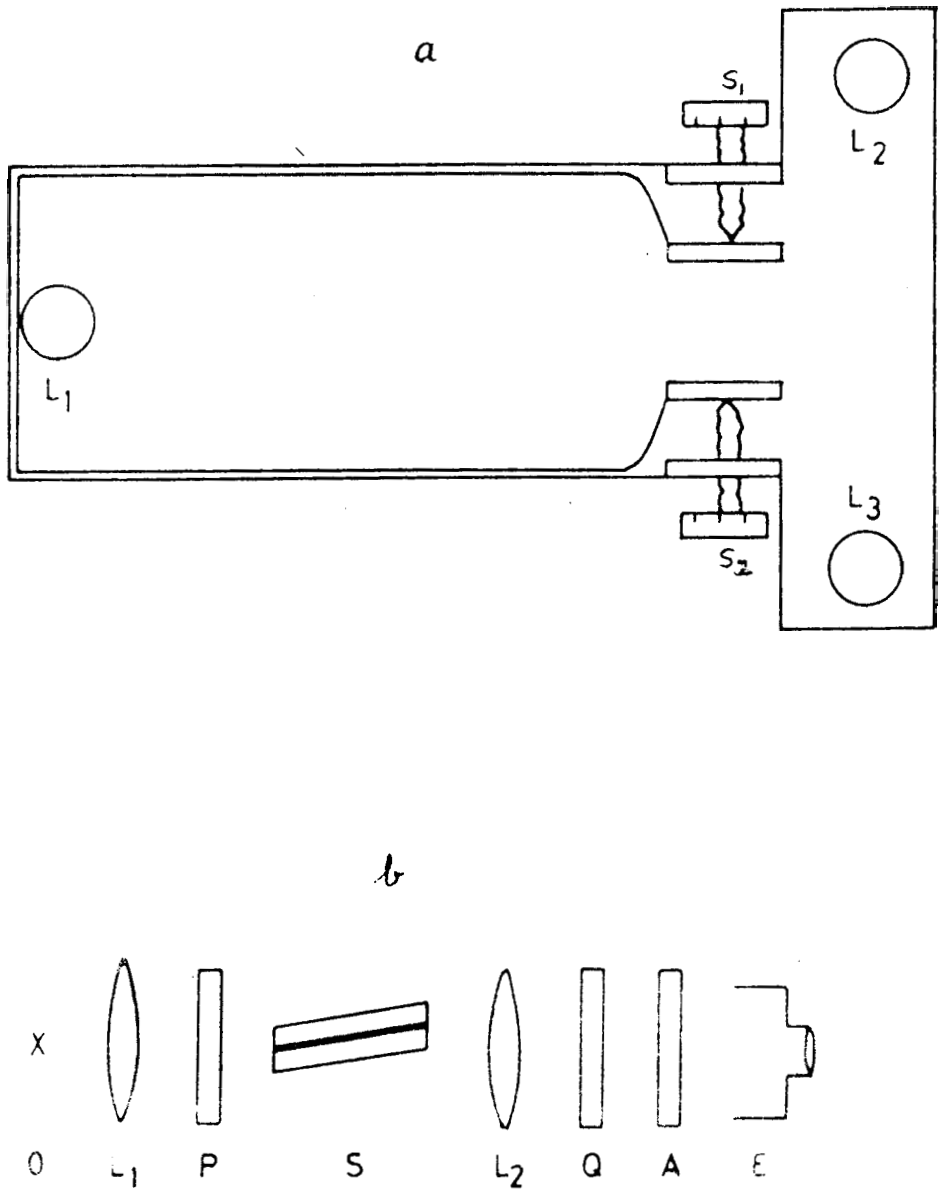

Figure 2.5

(a) The base for the heater provided with levelling screws L_1, L_2, L_3. The aide *screw.* are used to align the nematic director to be exactly normal to the magnetic field.

(b) Schematic diagram of the set up to detect optically the critical magnetic field for k_{22}.

Küstner Nacht K.G., East Germany). Since the thermo e.m.f. is not a linear function of temperature, a quadratic interpolation formula was used to calculate the temperature from the measured thermo e.m.f.

The hot junction was fixed to the sample holder so that it was in contact with *one* of the glass plates at its mid point. The cold junction was in contact with a massive copper block which in turn is placed in melting ice (made by using distilled water). The thermo e.m.f. was measured by a vernier potentiometer Type 30071 (The Oriental Science Apparatus Workshops India). The accuracy of temperature measurement was $\sim$ 0.02°C.

The temperature was controlled by passing a known current through the heater coil. A sufficient time (about half an hour) was allowed for the oven to come to an equilibrium temperature (within $\sim$ 0.02°C) before the measurements were taken.

(g) Optical set up: The light beam from a sodium vapour lamp is rendered parallel by lens L_1 (figure 2.5b). Linearly polarized light from a polarizer 3 set at 45° to the field direction is allowed to fall on the sample. The light emerging *from*

the sample is elliptically polarized. By using a quarter wave plate Q with its fast axis parallel *to* the axis of the polarizer, the elliptically polarized light is converted to ei linearly polarized one which is then viewed through the linear analyser A. The observation was made by focussing a low power microscope [shown in fig.2. with objective L_2 and eye piece E] onto a suitable region of the sample.

(h) Measurement of the magnetic field: A Hall probe gaussmeter (~ode%GH867 - Electronics Corporation sf India) wars used. The gaussmeter was calibrated against a NMR unit. The measurement of H was accurate to ~ ±25 gauss. The calibration of the magnetic field was also eheoked against the readings of another gaussmeter, Model 750, Radio Frequency Lab., U.S.A.

(i) Measurement of the critical field: To start with, the analyser was set to see a dark field of view. Observation was made on a small area (~ 1 mm^2) of the sample to reduce any errors due to temperature gradients and non-uniformity *3f* thickness. The magnetic fiold was increased until a weak deformation occurred in the sample. The *field of* view, then became bright. The magnetic field was then reduced in steps of ~ 25 gauss.

At each step a sufficiently long time was allowed so that the sample had enough time to relax. The magnetic field at which *the* field of view becomes dark was Oaken as *the* critical field. To verify that this is the correct critical field, the field was increased by 25 gauss and it was ascertained that the field of view became just bright.

Results and calculations

From equation (1.12) we have

$$k_{22} = \frac{H_c^2 x_o^2}{\pi^2} \Delta\chi \qquad (2.5)$$

$\Delta\chi$ is the anisotropy of volume diamagnetic susceptibility of the medium. We can write $\Delta\chi = \Delta\chi_{om} \cdot \rho \cdot S$ where S is the degree of orientational order of the medium, ρ is the density end $\Delta\chi_{om}$ is the anisotropy of the mass diamagnetic susceptibility of the perfectly oriented medium with S = 1. Hence

$$k_{22} = \frac{H_c^2 x_o^2}{\pi^2} \Delta\chi_{om} \cdot S \cdot \rho \qquad (2.6)$$

We have measured the twist elastic constant of two well known nematic compounds, namely, paraazoxyanisole

(PAA) and paraazoxyphenetole (PAP) for which all the relevant data are available.

(a) PAA: The order parameter S of PAA has been measured by a number of techniques. The values from optical anisotropy measurements (Chatelain and Germain 1964) calculated by Chandrasekhar and Madhusudana (1969) and Saupe (1968) agree well with each other. The values calculated from a molecular statistical model (Chandrasekhar and Madhusudana 1971) give a good fit with the experimental values. Moreover, the magnetic susceptibility anisotropy calculated using the theoretical values of S agree well with the experimental data of Gasparoux and Prost (1971). Hence we hare taken the S values f a our calculations from the theoretical curve.

Maier and Saupe (1960) have measured the temperature variation of density of PAA accurately. Chandrasekhar et al. (1969) have given an empirical relation

$$\rho = \rho_o \left(1 + \int_T^{T_{NI}} \alpha \, dT\right) \qquad (2.7)$$

where

$$\alpha = \frac{12.65 \times 10^{-4}}{(T_{NI} - T)^{1/6}}$$

to fit the experimental values. We used the relation (2.7) *to* obtain ρ at any temperature. The values of S and ρ st some temperatures are given in table 2.1 given at the end af this Chapter.

Foex (1933) measured the principal magnetic susceptibilities of the crystalline state of PAA. [X-ray studies on crystalline PAA show that the molecules are arranged in the lattice parallel *to* one another (Bernal and Crowfoot 1933)]. Hence the anisotropy of mass diamagnetic susceptibility of the medium with perfect orientation (S = 1) can be calm-lated ($\Delta\chi_{om} = 2.42 \times 10^{-7}$ c.g.s. units).

Using the above data re have calculated k_{22} for YAA at various temperatures. Table *(2.2)* contains the measured values of H_c and also k_{22}. The values obtained from two different samples are given separately.

Ignoring the changes in the molar volume with temperature, we have least square fitted k_{22} to the equation

$$k_{cal} = C\, S^x \qquad (2.8)$$

where C and x are free parameters. The best fit gives C = 15.73×10^{-7} and x = 1.99 $\approx$ 2. Hence the elastic constant values agree well with the mean field theory which predicts $k_{ii} \propto S^2$. The experimental points along with the calculated variation (Prom equation 2.8) are shown in figure 2.5.

(b) PAP: The values of S for PAP have been calculated from optical anisotropy measurements of Chatelain and Germain (1964), by Chandrasekhar and Madhusudana (1969) and by Saupe (1968). The experimental values agree well with the theoretical curve of Chandrasekhar and Madhusudana (1971). We have taken the theoretical values fox our calculations.

Bauer and Bernamont (1936) have made relative dilatometric measurements on PAP as a function of temperature. Their values are normalized to the absolute scale from the molar volume at T_{NI} (Maier and Saupe 1960). Chandrasekhar et al. (1969) have given an empirical relation (2.7) which fits the experimental values quite well. (Here $\alpha = \frac{13.03 \times 10^{-4}}{(T_{NI} - T)^{1/3}}$).

The S and ρ values at different temperatures are given in table 2.3.

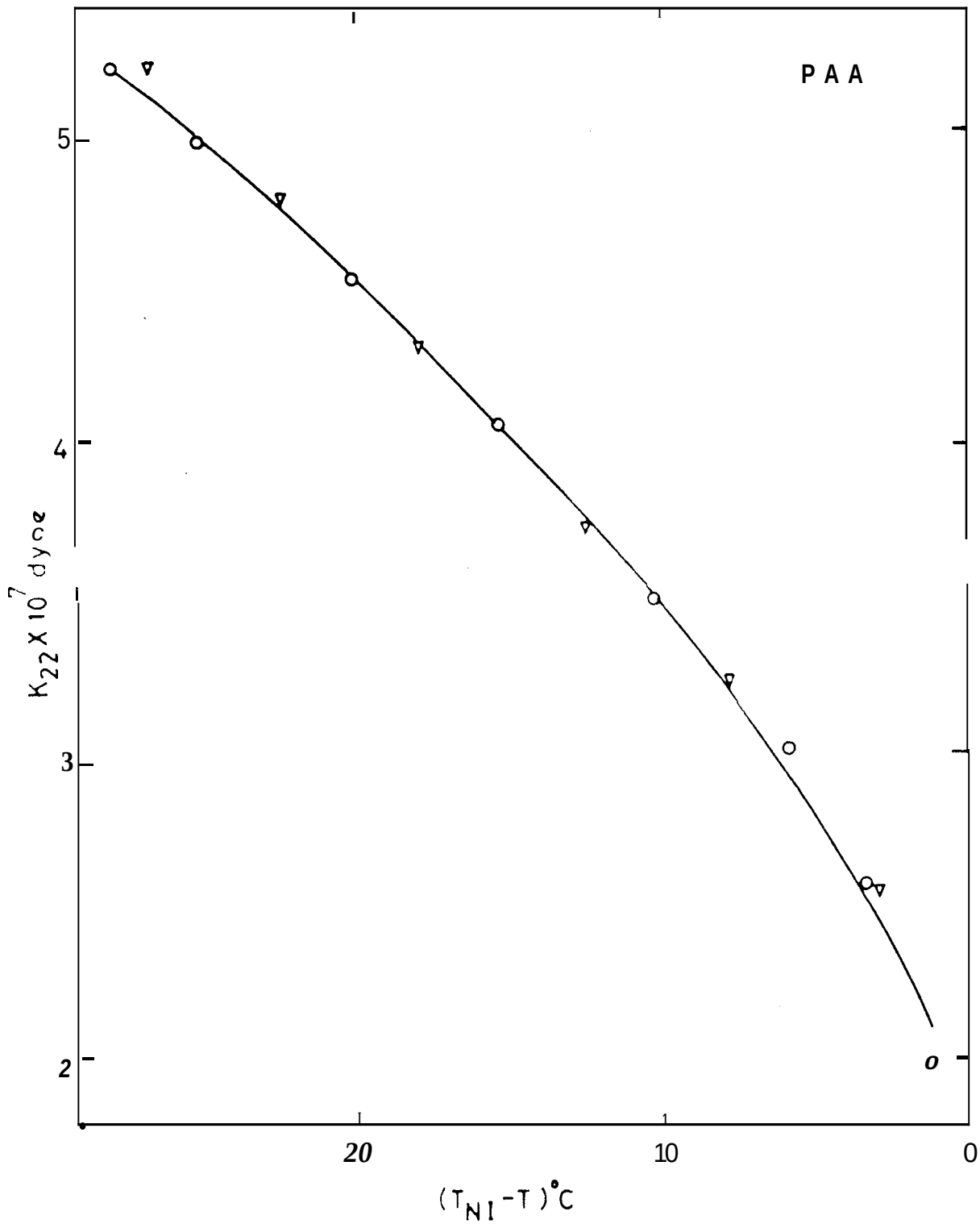

Figure 2.6

Twist constant vs. relative temperature (T_{NI} - T) for PAA. Circles and triangles represent measurements on two different samples.

Since the anisotropy of diamagnetic susceptibility arises essentially from the aromatic rings, we have assumed that the molar susceptibility of PAA and PAP are the same. Hence

$$\Delta\chi_{om}(PAP) = \frac{\Delta\chi_{om}(PAA)}{M_{PAP}} \cdot M_{PAA} \qquad (2.9)$$

where M_{PAA} and M_{PAP} are the molecular weights of PAA and PAP respectively. The calculated value of $\Delta\chi_{om}(PAP)$ is 2.19 x 10^{-7} c.g.s. e.m. units.

The tabla 2.4 gives the measured value. of H_c and the values of twist constant of PAP at various temperatures, calculated using the data compiled above. The values from three independent sets of measurements on different samples *are* given separately. The values of k_{22} are estimated to be accurate to ±5%.

The least squares fitting of the measured values of k_{22} to the equation (2.8) yields the results $C = 15.3 \times 10^{-7}$ and $x = 1.96 \approx 2$. Hence k_{22} values of PAP also are in good agreement with the mean field theory. The experimental values along with calculated variation from eqn. (2.8) are given in figure 2.7.

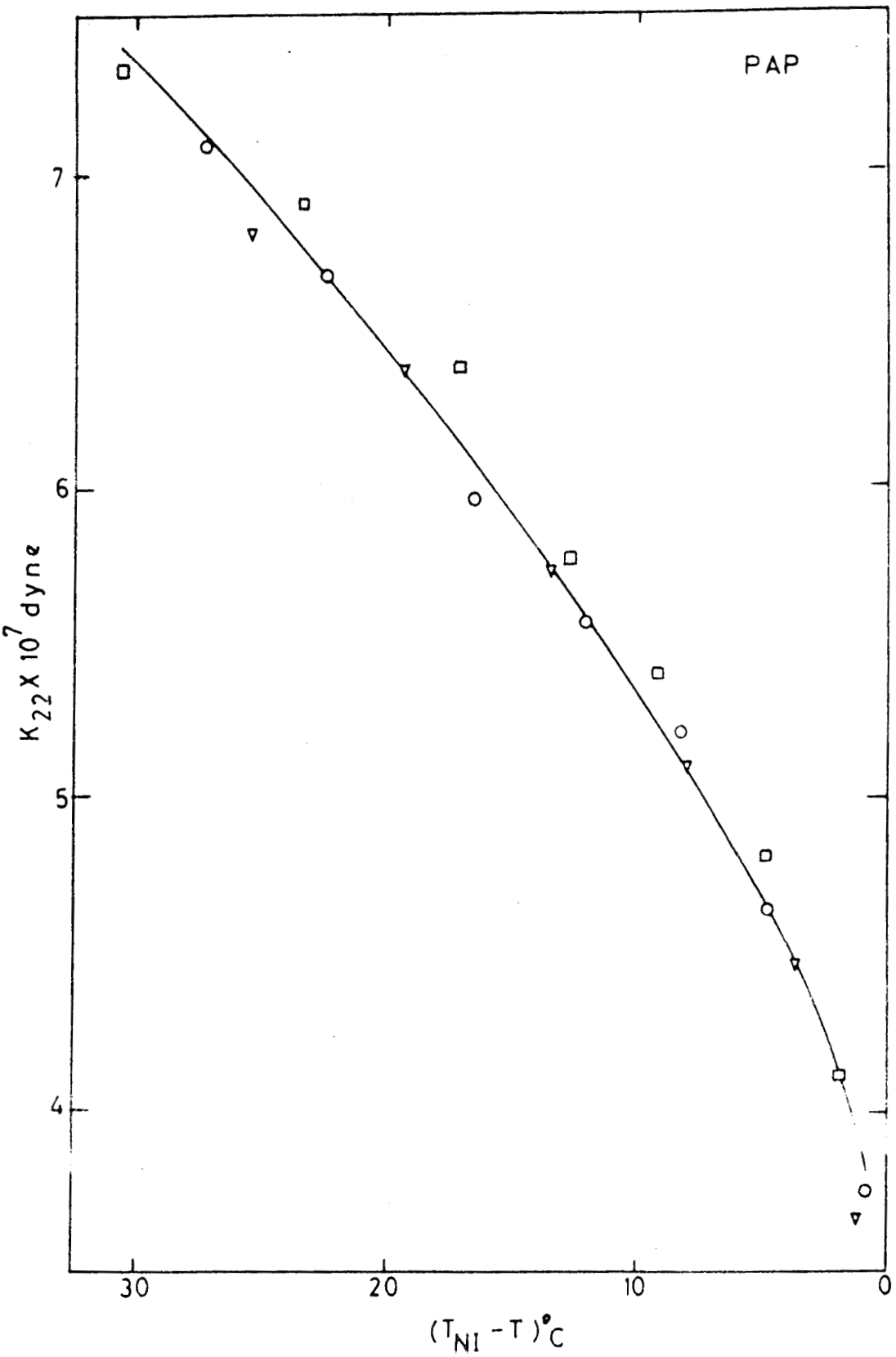

Figure 2.7

Twist constant vs. relative temperature for PAP. Circles, squares and triangles represent measurements on three different samples.

Discussion

The only values of k_{22} of PAA available for comparison with our experimental data are (1) measurements at different temperatures by Freedericksz and Zwetkoff (1934) which were used by Saupe (1960) to calculate k_{22}, (2) that at 129°C by Durand et al. (1969), and (3) that at 125°C by Leger (1572).

For the sake of comparison, the values given by the above authors are recalculated using the data on S, ρ and $\Delta\chi_{om}$ given above. The results are given in figure 2.8. It can be seen that the agreement of our values with those of earlier measurements is quite good. (Although Leger's value is slightly high (15%) it is within the error claimed by her.).

The only value of k_{22} for PAP available for comparison is that at 147°C by Durand et al. (1969) from the measurement of magnetic field induced cholesteric-nematic transition. This value is ~ 11% higher (within the accuracy of ±15% claimed by them) than our value at that temperature.

The temperature variation of k_{22} of both PAA and PAP are in agreement with the S^2 dependence. It implies that throughout the temperature range the molecular distribution function which would influence k_{22} does

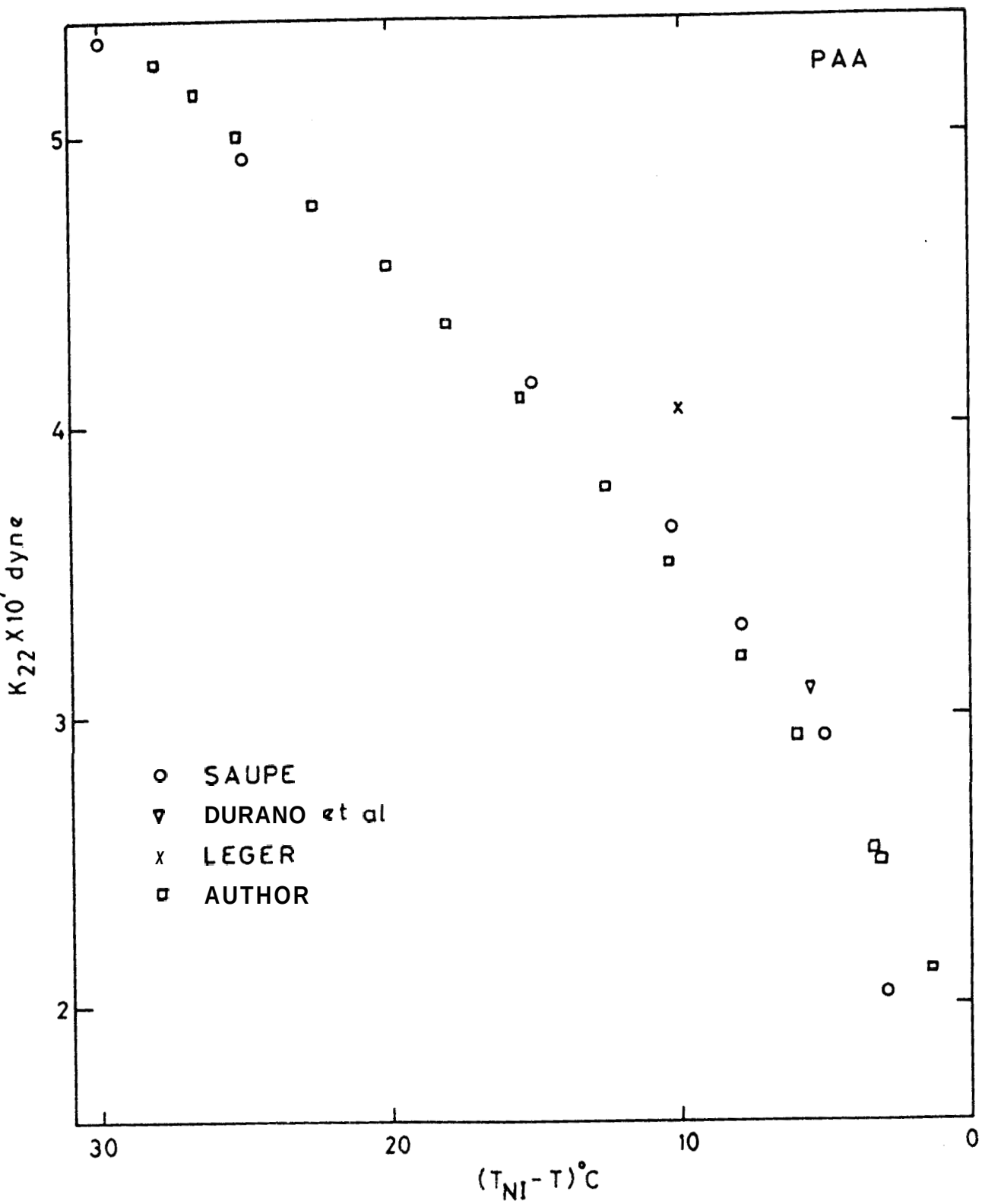

Figure 2.8

Twist constant vs. relative temperature for PAA obtained by other investigations recalculated as explained in the text.

not change. Comparing the values of C in PAA end PAP, we note that they are nearly equal. Hence in going from PAA to PAP the average distance between the molecular centres measured along the breadth of the molecules bas remained almost the same (Gruler 1975).

The dependence of the mean field potential on the molar volume is a matter of much discussion. For example, Maier and Saupe (1959) found the dependence of V^{-2}, Chandrasekhar et al.(1972) use V^{-3} dependence while Alben (1971) gets V^{-4} dependence. High pressure work of McColl and Shih (1972) seems to suggest V^{-4} dependence, while recently Cotter (1976) has argued that any mean field theory will be self consistent only with a V^{-1} dependence. We hare ignored the volume dependence in our calculations of k_{cal}. Since the change in the molar volume ovsr the entire temperature range is only $\sim 2\%$ the results *ore* not drastically altered

We may compare our measurements on k_{22} with the bend and splay constants measured by Gruler (1973). In PA* k_{33} varies more rapidly than that given by an S^2 dependence, while k_{11} satisfies an S^2 dependence. As we shall see in Chapters III and IV, k_{33} does not

obey mean field theory in almost all the other compounds studied.

Conclusions

(1) The new method to determine the twist elastic constant, employed hero, gives consistent values for independent samples. Moreover they agree well with those measured from other methods. Hence the present method is quite reliable.

(2) The twist constant of both PAA and PAP obey tho mean field theory. Hence the structure of the short range order relevant to k_{22} does not change throughout the temperature range.

(3) The values of C In equation (2.8) are almost equal for PAA and PAP. Hence the nature of the short range order is rather similar in the two cases.

References

Alben, R. 1971 Mol. Cryst. Liq. Cryst. 13, 193.

Bauer, E. and Bernamont, J. 1936 J.Phys.Radium 7, 19.

Bernal, J.D. and Crowfoot, D. 1933 Trans. Faraday Soc. , 1032.

Chandrasekhar, S. and Madhusudana, N.V. 1 6 J. de Physique 30, C4-24.

Chandrasekhar, S., Krishnamurthy, D. and Madhusudana, N.V. 1969 Mol.Cryst.Liq.Cryst. 8, 45.

Chandrasekhar, S., and Madhusudana, N.V. 1971 Acta Crystallogr. 27A, 303.

Chandrasekhar, S., Madhusudana, N.V. and Shubha, K. 1572 Acta Crystallogr. , 28.

Chatelain, P. 1943 Bull.Soc.Fr.Miner. 66, 105.

Chatelain, P. and Germain, M. 1964 C.R.Acad.Sci. Paris 259, 127.

Chu, K.C. and McMillan, W.L. 1975 Phys.Rev. A11, 1059

Cladis, P.E. 1972 Phys.Rev.Lett. 28, 1629.

Cotter, M.A. 1976 (to be published).

de Gennes, P.G. 1968a C.R.Acad.Sci.Paris 266, 15.

de Gennes, P.G. 1968b Solid State Commun. 6, 163.

de Gennes, P.G. 1971 J. de Phys. 32, 789.

de Gennes, P.G. 1574 'Physics of Liquid Crystals' Clarendon Press, p. 88.

Delaye, M., Ribotta, R. and Durand, G. 1973
Phys. Rev. Lett. 31, 443.

Delaye, M. 1976 (to be published).

Ditchburn, R.W. 1952 'Light', Blackie and Son Ltd. p.141.

Dreher, R. 1974 Z. Naturforsch. 29a, 125.

Durand, G., Leger, L., Rondelez, F. and Veyssie, M.
1969 Phys. Rev. Lett. 22, 227.

Foex, G. 1 Trans. Faraday Sou. 29, 958.

Freedericksz, V. and Zwetkoff, V. 1934 Phys. Z. Soviet
Union, 6, 490.

Gasparoux, H. and Prost, J. 1971 J. de Phys. 32, 65

Gerritsma, C.J., de Jeu, W.H. and Van Zanten, P. 1971
Phys. Lett. 36A, 389.

Gruler, H. 1973 Z. Naturforsch. 28a, 474.

Gruler, H. 1975 Z. Naturforsch. 30a(2), 230.

Haller, I. 1972 J. Chem. Phys. 57, 1400.

Helfrich, W. 1970 Appl. Phys. Lett. 17, 531.

Hurault, J.P. 1973 J. Chem. Phys. 59, 2068.

Leenhouts, F., Van der Wonde, F. and Dekker, A.J.
(Private communication).

Leger, L. 1972 Solid State Commun. 10, 697.

Leslie, F.M. 1970 Mol. Cryst. Liq. Cryst. 12, 57.

Maier, W. and Saupe, A. 1959 Z.Naturforsch. 14a, 882.

Maier, W. and Saupe, A. 1960 Z. Naturforsch. 15a, 287.

McColl, J.R. and Shih, C.S. 1972 Phys.Rev.Lett. 29, 85.

Meyer, R.B. 1968 Appl. Phys. Lett. 14, 208.

Meyer, R.B. 1971 Colloq. Liq. Cryst. Pont-a Mousson.

Orsay Liquid Crystal Group 1969 J.Chem.Phys. 51, 816.

Rapini, A and Papoular, M. 1969 J. de Physique 30, C4-54.

Rondelez, F. and Hulin, J.P. 1972 Solid State Commun. 10, 1009.

Saupe, A. 1960 Z. Naturforsch. 15a, 815.

Saupe, A. 1968 Angew. Chem. Internat. Edit. 7, 97.

Williams, C. and Cladis, P.E. 1972 Solid State Commun. , 357.

Table 2.1

Order parameter and density of PAA

$T_{NI} - T$ in °C	S	ρ gm/cc
0.5	0.347	1.1486
1.0	0.359	1.1493
4.0	0.408	1.1531
7.0	0.442	1.1564
12.0	0.485	1.1614
17.0	0.519	1.1661
27.0	0.571	1.1748
37.0	0.612	1.1829

Table 2.2: Twist elastic constants of PAA

$T_{NI}-T$ in °C	Ho in Kgauss	k_{22}x107 dynes	$k_{cal}=0S^{x}$x 10^{7} dyne
26.7	4.5	5.23	5.14
22.3	4.4	4.79	4.76
17.9	4.275	4.31	4.35
12.5	4.125	3.72	3.78
7.8	4.025	3.24	3.19
3.0	3.8	2.53	2.48
x_o = 12.5 µm			
27.9	0.945	5.22	5.25
25.1	0.935	4.98	5.00
20.1	0.915	4.53	4.55
15.4	0.890	4.05	4.09
10.3	0.860	3.49	3.52
5.9	0.840	3.02	2.92
3.3	0.805	2.57	2.53
1.2	0.740	1.98	2.11
x_o = 59.4 µm.			

Table 2.3

Order parameter and density of PAP

$T_{NI}-T$ °C	S	ρ gm/cc
1	0.499	1.070
2	0.515	1.072
4	0.535	1.074
8	0.570	1.078
13	0.604	1.083
18	0.632	1.088
28	0.680	1.098
37	0.709	1.106

Table 2.4: Twist elastic constant of PAP

$T_{NI}-T$ °C	H_c in Kgauus	$k_{22}x10^7$ dynes	$k=CS^x x10^7$ dynes
27.2	2.625	7.06	7.12
22.1	2.60	6.66	6.65
16.4	2.525	5.95	6.05
12.1	2.50	5.56	5.56
8.3	2.475	5.21	5.12
4.8	2.40	4.65	4.66
0.8	2.275	3.78	3.87
x_o = 25.0 µm			
25.4	0.655	6.80	6.96
19.3	0.65	6.37	6.38
13.5	0.635	5.72	5.73
8.0	0.62	5.10	5.08
3.7	0.60	4.47	4.49
1.3	0.56	3.66	4.01
x_o = 99.0 µm			
30.8	0.885	7.32	7.41
23.8	0.88	6.89	6.81
17.6	0.87	6.37	6.18
12.6	0.85	5.77	5.62
9.0	0.84	5.40	5.21
4.7	0.82	4.83	4.64
1.9	0.78	4.12	4.15
x_o = 74.6 µm			